

THIRTEENTH EUROPEAN ROTORCRAFT FORUM

7.6  
Paper No. 61

CORRELATION OF GENERALIZED HELICOPTER FLIGHT TEST  
PERFORMANCE DATA WITH THEORY

K. LIESE, J. RUSSOW, G. REICHERT

TECHNICAL UNIVERSITY OF BRAUNSCHWEIG  
BRAUNSCHWEIG, GERMANY

September 8-11. 1987

ARLES, FRANCE

CORRELATION OF GENERALIZED HELICOPTER FLIGHT TEST  
PERFORMANCE DATA WITH THEORY <sup>†</sup>)

K. Liese  
J. Russow  
G. Reichert

Technical University of Braunschweig  
Braunschweig, Germany

Abstract

Data from helicopter performance tests are scattered and moreover, the flight-test-conditions differing in temperature and altitude have to be considered. Thereby the direct correlation to results of performance calculations and theory is complicated.

Data reduction allows to concentrate the test data to few generalized parameters derived from momentum theory and simularity methods. Subsequent computation of an adjustment eliminates the scattering and creates definite relations, which are shown for hover and forward flight with climb and descent including autorotation. This allows the determination of power required from test data avoiding random errors.

Correlation with the results of performance calculations is then done on the generalized basis, reducing the number of flight conditions to be checked.

Notation

a	[m/s]	Speed of sound	$V_h$	[m/s]	Horizontal flight velocity
g	[m/s <sup>2</sup> ]	Gravity constant	$V_v$	[m/s]	Climb velocity
$K_G$	[-]	Weight coefficient $\frac{m g}{\frac{\rho}{2} U^2 S}$	$\bar{V}_h$	[-]	Nondimensional horizontal velocity $\bar{V}_h = \frac{V_h}{w_{iS}}$
$K_P$	[-]	Power coefficient $\frac{P}{\frac{\rho}{2} U^3 S}$	$\bar{V}_v$	[-]	Nondimensional climb velocity $\bar{V}_v = \frac{V_v}{w_{iS}}$
$K_{PS}$	[-]	Power coefficient in hover	$w_{iS}$	[m/s]	Main rotor induced velocity in hover
m	[kg]	Helicopter mass	$X_p$	[-]	Power factor
$Ma_U$	[-]	Mach number of rotor tip speed $Ma_U = \frac{U}{a}$	$\lambda_h$	[-]	Horizontal advance ratio $\lambda_h = \frac{V_h}{U}$
P	[Nm/s]	Power required	$\lambda_v$	[-]	Vertical advance ratio $\lambda_v = \frac{V_v}{U}$
R	[m]	Rotor radius	$\rho$	[kg/m <sup>3</sup> ]	Air density
S	[m <sup>2</sup> ]	Rotor disc area $S = \pi R^2$	$\omega$	[1/s]	Main rotor rotational speed
U	[m/s]	Rotor tip speed $U = \omega R$			

<sup>†</sup>) Work sponsored by the Ministry of Research and Technology of the Federal Republic of Germany

## 1. Introduction

Helicopter flight test data are an evident assumption for developing performance prediction methods and for demonstrating compliance with certification requirements /1,2,3/. Since tests need considerable costs and time, one usually makes an effort to reduce them to a minimum.

On the other side there are numerous physical parameters found for determination of power required, the influence of which must be taken into consideration. They are atmosphere data as well as parameters of the helicopter itself which define its state of flight. In order to describe the connection between power required on the one hand and the influencing parameters on the other, a multi-dimensional data field would have to be established. For the flight tests as well as for numerical or graphical presentation of the result, it is a problem that cannot be solved. When this point of problem is reached, the methods of the data reduction become important /4-16/.

The application of data reduction methods leads to a clear presentation of power required, decreasing the number of flight conditions to be investigated. The method for the data reduction applied here is a further development of the methods already established. The historical development of the data reduction for helicopters is shortly presented in the next chapter.

When evaluating the performance flight tests, a further problem arising are the scattering of the test data resulting from a not complete stationary flight state, especially since in numerous flight states a helicopter is unstable which always requires control interventions, p.ex. during atmosphere disturbances. Moreover, mistakes (like drifts and hysteresis) and incorrectnesses of sensors or due to analogous data registration cannot be excluded. The numerical interpretation of a physical relation as well as the comparison with calculation results are made more difficult by deviations. Thus it is necessary to extinguish the scattering by applying adequate mathematical procedures.

At last, the result is a presentation in few diagrams of power required of a helicopter during stationary hover and forward flight with climb and descent including autorotation. The test results are shown as adjustment curves leading to a definite mathematical description of the data.

## 2. Historical Survey on the Development of Data Reduction Methods

The first performance reduction methods especially for helicopters were published shortly after the second world war /4-6/. In those years, helicopters were equipped with piston engines that did not allow direct measurements of the present power.

This way the engine and its dependence on outer conditions is included in the investigations. The performance results were often presented in form of p.ex. maximum speed, or maximum climb that the helicopter could reach under certain conditions. Data reduction meant converting them into other (mostly standardized) atmosphere conditions. This conversion was done with the help of the same equations also applied to performance calculations /4/.

This changed when turbine engines fitted with torquemeters were introduced /7/. By this way, the power available of the engine could be considered irrespectable of the power required of the helicopter. Today, this is the decisive parameter for the definition of the performance.

For the performance reduction methods this means a change, too. A helicopter is a fluid machine like a turbine engine. Its forces, moments and power are represented by non-dimensional parameters that can be deducted by dimensional analysis. After LANGDON /7/ had presented this description for the turbine engines in 1961, he suggested corresponding parameters for the helicopter in the same year /8/. In the following years, these methods were taken up by FISHER /9/ and KNOWLES /10/ and have been made use of by the Engineering Science Data Unit /11,12,13/ since 1973.

In order to describe the conditions during hover OGE and IGE /12/, the data reduction by dimensional analysis is sufficient. However, for the horizontal flights /13/ three independent parameters remain in connection with the corresponding problems regarding presentation and interpretation of the results. For a continued reduction the pure dimensional analysis is therefore not sufficient, especially as regards forward flights with climb and descent. By adding information about the physics of helicopter flight like momentum theory, BOIRUN /14/ managed to include these flight cases too, in simple diagrams. A similar but more empirical method was applied by SMITH /15/.

These methods are the basis for the reduction used in this paper including some modifications explained in detail in the next chapter.

### 3. The Data Reduction

The complexity of a physical or technical system is especially represented by the number of occurring state or influencing variables. Even if all the important influencing parameters of a system are known by measurements or calculations, it is often impossible to carry out a numerical description. The dimensionality of the data field rises with an increasing number of the parameters.

This has a growing number of measurement points as a consequence which are necessary to fill the data field. Above all, there is no longer the possibility of analyzing the position of the measurement values by a graphic representation.

The data reduction takes an interest in this problem by reducing the number of variables necessary for the description of the problem with the help of different measures. In the following, suitable methods for the clear description of power required of a helicopter are presented.

#### 3.1 Determination of the Non-Dimensional Parameters

The marginal conditions for the stationary helicopter flight OGE are described by six independent variables.

- helicopter weight  $mg$  [N] or  $[kg \ m/s^2]$
- rotor tip speed  $U$  [m/s]
- horizontal velocity  $v_h$  [m/s]
- vertical velocity  $v_v$  [m/s]
- air density  $\rho$  [kg/m<sup>3</sup>]
- speed of sound  $a$  [m/s]

The dependent variable that is to be presented is the power required:

- power required  $P$  [Nm/s] or  $[kg \ m^2/s^3]$

In systems where influencing variables occur in different units, dimensional analysis and dynamic similarity methods are useful to classify the variables involved /18-21/. It should be kept in mind that a study of dimensions by itself does not yield any information about the physical phenomena or the function relation between the variables involved. A study of dimensions, however, frequently aids in making an easier and more convenient description of the phenomena /21/.

Describing by non-dimensional parameters means at the same time eliminating the absolute geometrical size of the system. Therefore, a characteristic measurement of the helicopter is necessary in order to allow a corresponding reference. For this purpose, the rotor radius is used in

most of the cases:

- rotor radius  $R$  [m]

The variables and exponents of the units are summed up in the matrix presented in Table 1.

There are  $n=8$  dimensional variables. As a pure fluid mechanic system is the question, the number of the physical basic units is  $m=3$ . The rank of the matrix is  $r=3$ . Therefore,  $n-r=8-3=5$  physical similiarity parameters do exist /19/ for the description of the proceedings in the system. One parameter is needed for the description of power required, whereas the remaining four define the non-dimensional marginal conditions. One of many possibilities to create these five parameters is shown in Table 2.

By choosing these parameters the flight state is clearly described. The parameters are the relations of two equal physical variables as for instance advance ratio = velocity/velocity or weight coefficient = force/force. By making use of the dimensional analysis we succeeded in reducing the system of 6+1 influencing variables (6 independent, 1 dependent) to a system of 4+1 non-dimensional parameters.

It is not possible to show 5 parameters in one diagram. This is why further steps must follow in order to reduce the data even more.

### 3.2 Restriction to Hover

As well-known possibility to reduce the number of the parameters is the consideration of certain flight states. For a helicopter, the state of hovering should be regarded because then both the advance ratios are zero. Thus the system of these parameters is further reduced from 4+1 to 2+1. Henceforth, the numerical dependence between power coefficient and weight coefficient as well as the Mach number at the blade tip is wanted. This connection can now be established by flight tests or performance calculations. The graphical presentation shows a family of curves in a two-dimensional plotting. Such a diagram or characteristic field is a common plotting for the function of three parameters. Fig. 1 shows the calculated power required in hover as a plotting of the three non-dimensional parameters.

The power coefficient increases non-linearly with the weight coefficient. A rise of the rotor Mach number increases the dimensionless power required also non-linearly /8-12/.

The parameters  $K_G$  and  $K_p$  must be seen in connection with the physics of a fluid machine, i.e. the forces (thrust) are quadratically dependend on the occurring velocities, in this case the blade tip velocity  $U$ . The power is a cubic function of  $U$ . The size of the helicopter is characterized by the rotor area  $S$ , the density  $\rho$  considers the atmosphere.  $Ma_0$  is a similiarity parameter for the influence of the compressibility.

The reduction is not complete if kinds of power occur that do not follow the regularities mentioned above, for instance a constant power for the drive of a generator or power loss that is non-linear to the power fed in, p. ex. in the gear-box.

Further effects that are not considered in the hover diagram are the Reynold and the Froude similarities. The Reynold number is an index for the friction forces due to the viscosity of air; the Froude number, for example, influence the conus angle of the rotor. It is well known, that the effects of these parameters can be neglected as long as they do not change in orders of magnitude; this is the case for smaller wind tunnel models.

Both the parameters would result from the dimensional analysis if, on the one hand, mass  $m$  and acceleration due to gravity  $g$  appear singularly and on the other hand the viscosity of the air

is added to the list of influencing variables. To sum it up we can therefore say that for the special situation of hover the dimensional analysis offers a satisfying presentation of power required in one diagram.

### 3.3 Extension to Forward Flight with Climb and Descent

In forward flight with climb or descent two further influencing variables are needed in order to define the flight state. This concerns the horizontal and vertical flight velocity, the non-dimensional parameter horizontal and vertical advance ratios  $\lambda_h$  and  $\lambda_v$ , respectively, corresponding to the dimensional analysis mentioned above. Thus, the four independent parameters are involved (see chapter 3.1). It is impossible neither to find out this relationship nor to show it (graphically) at an adequate expense. Therefore, data reduction must limit the dimensionality in a way that at the most 2+1 parameters are left over.

The solution of the problem results from the fact that the parts of helicopter power required are considered physically including the hover diagram presented above. If the hover diagram is extended over the flyable range to  $K_G=0$ , conclusions can be drawn as regards the power parts see Fig. 2.

If the helicopter is run at about zero thrust at the ground, the constant power can be measured at  $K_G=0$  which essentially consists of power required for profile drag of main and tail rotor /16/.

In case that the thrust of the rotor is increased, the variable part  $\Delta K_{PS}(K_G)$  is added which primary results from the induced powers of rotors. The course of  $K_{PS}$  can be described as follows:

$$K_{PS} = K_{PS}(K_G=0) + \Delta K_{PS}(K_G) \quad \text{and} \quad \Delta K_{PS} \sim K_G^n$$

With  $n > 1,5$  due to power of the tail rotor. The forward flight with climb and descent (as well as the ground effect /16/) has an impact on the variable power /14/. Therefore, it is obvious to define a power factor  $X_P$  that is multiplied with the variable power part  $\Delta K_{PS}$ :

$$K_P = K_{PS}(K_G=0) + X_P \Delta K_{PS}(K_G)$$

The variables  $K_{PS}(K_G=0)$  and  $\Delta K_{PS}$  are known from the hover diagram. In order to consider the horizontal and vertical velocities, the factor  $X_P$  has to be defined. Therefore, the first question arising is by which non-dimensional parameters the velocities are to be described. Regarding the dimensional analysis of the complete system, the advance ratios  $\lambda_h$  and  $\lambda_v$  were the result. They were applied as parameters in a number of reduction methods /8-13/. However, it is obvious that with these parameters a complete reduction is not possible as the influence of  $K_G$  on the velocity axis continues to exist.

On the other hand, CHEESEMAN and BENNETT /17/ as well as BOIRUN /14/ use the average induced velocity of the main rotor during hover  $w_{is}$  as a reference variable for the velocities:

$$\bar{v}_h = \frac{v_h}{w_{is}}$$

$$\bar{v}_v = \frac{v_v}{w_{is}}$$

In this respect they are similarity parameters that can be deduced from the momentum theory. The change of the induced power when the helicopter is moving results from the momentum theory which does obviously not depend on the tip speed of the rotor. The calculation of the average induced velocity of the rotor during hover is done according to the well-known formula:

$$w_{iS} = U \sqrt{K_G/4} = \sqrt{\frac{mg}{2\rho S}}$$

As a consequence, the non-dimensional velocities can be described as:

$$\bar{v}_h = \frac{v_h}{U \sqrt{K_G/4}} = \frac{\lambda_h}{\sqrt{K_G/4}}$$

$$\bar{v}_v = \frac{v_v}{U \sqrt{K_G/4}} = \frac{\lambda_v}{\sqrt{K_G/4}}$$

This way, the two non-dimensional parameters represent a combination of two parameters each which were deduced from dimensional analysis. The relations mentioned above allow the following model for power required during forward flight with climb and descent:

$$K_P(K_G, Ma_U, \bar{v}_h, \bar{v}_v) = K_{PS}(K_G=0, Ma_U) + X_P(\bar{v}_h, \bar{v}_v) \Delta K_{PS}(K_G, Ma_U)$$

$$X_P(\bar{v}_h, \bar{v}_v) = \frac{K_P(K_G, Ma_U, \bar{v}_h, \bar{v}_v) - K_{PS}(K_G=0, Ma_U)}{\Delta K_{PS}(K_G, Ma_U)}$$

By this procedure, the additional influence of the flight velocity on power required can be shown by the function  $X_P = f(\bar{v}_h, \bar{v}_v)$  resulting in a family of curves in a plane, analogously to the hover diagram. Fig. 3 shows such a plotting carried out with calculated data.

The curves show the typical course of the power over the horizontal velocity. The climb or descent velocity leads to a distortion and shifting of the position. Autorotation results in slightly negative  $X_P$ .

This model meets the plan of BOIRUN /14/ and SMITH /15/ to eliminate the weight coefficient as an independent variable in forward flight tests. Compared with the methods used by BOIRUN /14/ the main difference is the determination of the variable (induced) power from the hover diagram, because in our own tests the assumption of an induced power increasing with the exponent 1.5 did not lead to a satisfactory reduction at different weight coefficients for helicopters with tail rotors.

As reported by BOIRUN /14/, there are additional effects of  $K_G$  and  $Ma$  in high speed flight. This leads to the fact that a complete reduction of the data in the curves presented does not occur. This is a matter of the influences of the retreating blade stall and compressibility at the advancing blade. If need is, these additional powers can be taken into consideration by corresponding additions. This case is not to be discussed here.

#### 4. Numerical Evaluation of the Flight Test Data

##### 4.1 Hover Flight

The determination of power required during hover flight is the basis of the performance analysis of a helicopter. When finding out the hover performance, the required exactness is in contrast to the fact that the flight state is relatively unsteady and thus requires constant

control interventions. Control of the flight velocity is eminently important, too, but a problem especially as regards helicopters. Therefore, these tests are mostly carried out with ground references, while the wind velocity is smaller than 2 Kts.

Fig. 4 shows the results of the hover tests with a BO 105 helicopter of the DFVLR in Braunschweig, plotted in the hover diagram according to chapter 3.2.

The points show the well-known course of the power coefficient over the weight coefficient. The Mach numbers as a consequence of the blade tip speed are marked by the signs. The test data can be found in the  $K_G$  range of 8 to  $12 \cdot 10^{-3}$  as well as of  $K_G = 0$  due to the ground tests. On the whole, the Mach numbers  $Ma_U$  are rather small. The reason is that there were not any tests carried out at extremely low temperatures.

The points show a scattering. The influence of the Mach number is smaller than the dispersion and thus cannot be clearly identified. This is why for the evaluation presented here we renounce the influence of the Mach number and just determine the dependence of parameter  $K_G$ . The curve is coordinated to the average Mach number of 0.64. Its mathematical determination requires a computation of an adjustment that approximates the points for instance by a polynome. The results of this calculation are the respective polynome coefficients:

$$K_{PS} = A_0 + A_1 K_G + A_2 K_G^2 + \dots + A_i K_G^i$$

The applied calculation programme determines the coefficients in a way that the average square deviation of the points is minimized. The degree to be chosen for the polynome depends on the course of curves to be imitated and can be determined when the data are evaluated. The degree should be increased step by step until a reduction of the average distance of the points does no longer occur.

Fig. 5 shows the hover diagram with the polynome of second degree.

As a consequence, a definite mathematical correlation between the parameters has been established by the adjustment curve. The power parts of the hover flight defined in chapter 3.3 can be determined with the help of the polynome

$$K_{PS}(K_G=0) = A_0$$

$$\Delta K_{PS}(K_G) = A_1 K_G + A_2 K_G^2 + \dots + A_i K_G^i$$

These are made further use of the evaluation of the forward flight data to follow.

#### 4.2 Forward Flight

At this point it is the horizontal forward flight that is to be considered in the first instance. Therefore, a plotting  $x_p$  over  $\bar{v}_h$  is concerned that was deduced in chapter 3.3. The flight data reduced correspondingly are shown in Fig. 6. From the position of the points the course of power required over the velocity is already obvious. Compared with the course on the whole, the scattering of the points seems to be only small. The marks of the test points reveal the range of the weight coefficient  $K_G$ . In order to chose the test data for the horizontal forward flight, the definition of a limit for the vertical velocity is necessary. That was set in a way that the absolute value of  $v_v$  measured during the test had to be smaller than 0.15 m/s.

In low to average range of velocity no  $K_G$  influence can be noticed, thus the data reduction (elimination of  $K_G$  out of the forward flight diagram) can be regarded as successful. It is



only in the range of high velocity that a tendency can be suspected. As already hinted in chapter 3.3 additional effects result here leading to a splitting according to value  $K_G$  and  $\lambda_h$ . Due to the small number of test data in this range it is only the main direction of the effects than can be determined.

A compensation curve can be calculated for the horizontal forward flight. In doing so, test points in the range of the highest velocities should only be considered with small weight coefficients and small Mach numbers. This results in the so-called unstalled baseline curve /14/. A polynome of fifth degree is sufficient to describe this curve which is plotted together with the test data in Fig. 7.

The vertical climb and descent can as well be regarded analogously to the horizontal forward flight. Then, a plotting of  $X_p$  over  $\bar{V}_v$  is the result with an adjustment curve that can be of smaller degree. This case is not regarded furthermore.

#### 4.3. Forward Flight with Climb and Descent

Fig. 8 shows the combination of  $\bar{V}_h$  and  $\bar{V}_v$ , which occurred at the flight tests.

The diagram also includes the hover flights at  $\bar{V}_h = \bar{V}_v = 0$  presented above. The horizontal flights have already been presented, too; they can be recognized along line  $\bar{V}_v = 0$ . The range of the vertical velocities  $\bar{V}_v$  is limited at the top by power available and at the bottom by autorotation. There is no regular distribution of the points over the area due to the bended course of the boundary.

As a result of the flight tests, Fig. 9 shows the power factor  $X_p$  as a function of  $\bar{V}_h$  and  $\bar{V}_v$ :

In this plotting, the parameter  $\bar{V}_v$  is represented by the sign that is coordinated to one range each. The valid area of the signs is marked in the diagram. Due to the lack of graphic clearness, the presentation of the  $K_G$  values is renounced.

The course of the curve at about  $\bar{V}_v = 0$  corresponds to that already presented in Fig. 6. It is evident that the power factor increases with climb velocity and decreases during descent. However, definite values cannot be read from the diagram. This is why for a mathematical description a regression calculation is carried out with the test data. In contrast to the situation mentioned before, this concerns a three-dimensional function  $z = f(x,y)$ .

With  $i$  as degree of the polynome in  $x$  direction and  $j$  in  $y$  direction, the following equation results:

$$\begin{aligned}
 z(x,y) = & \\
 & + B_{0,0} + B_{0,1} y + B_{0,2} y^2 + \dots + B_{0,j} y^j \\
 & + B_{1,0} x + B_{1,1} xy + B_{1,2} xy^2 + \dots + B_{1,j} xy^j \\
 & \cdot \quad \cdot \quad \cdot \quad \cdot \\
 & \cdot \quad \cdot \quad \cdot \quad \cdot \\
 & \cdot \quad \cdot \quad \cdot \quad \cdot \\
 & + B_{i,0} x^i + B_{i,1} x^i y + B_{i,2} x^i y^2 + \dots + B_{i,j} x^i y^j
 \end{aligned}$$

Therefore, a number of  $(i+1) \cdot (j+1)$  coefficients have to be determined. Compared with the two-dimensional situation mentioned in chapters 4.1 and 4.2 the algorithm for the calculation of the coefficients here is extended to the third dimension. Furthermore, the average square deviation of the test data from the adjustment area is minimized. The result is calculated by solving an equation system (non-iteratively).

Fig. 10 presents the result of the regression calculation.

The course of  $X_p$  over  $\bar{v}_h$  has been calculated from the coefficients for definite values of  $\bar{v}_v$ . The degree of the polynome is  $i=5$  and  $j=4$ .

One important advantage of this three-dimensional regression is the fact that the test data can be applied with different combinations of horizontal and vertical velocity. Subsequently, the power factor can be recalculated for any values of  $\bar{v}_h$  and  $\bar{v}_v$  within the valid range of the data.

When calculating values belonging to  $\bar{v}_h - \bar{v}_v$  combinations that are not in the investigated range one ought to be cautious. Such an extrapolation is not permissible. The course of the curves in the range  $\bar{v}_h = 0$  is an example in Fig. 10. Extrapolation into range of  $\bar{v}_v < 0$  would lead to an increasing power required although the course should have to be symmetrical to the axis.

On the whole, such a 3-D-regression calculation can cause problems because of numerical instabilities. One must pay special attention to the points in the investigated area to be distributed reasonably. Regarding this problem, the test results in Fig. 8 and 9 do not represent an ideal situation. It is true, however, that the number of 393 points is more than sufficient, but on the other hand their concentration near the boundaries is rather small. Therefore, the results presented here are to be considered as a first step to calculate a clear numerical description of the test values.

##### 5. Correlation of Flight Tests and Performance Calculation

The characteristic lines or fields established in chapter 4 by means of the regression calculation can be directly compared with the plottings presented in chapter 3. This can be easily done entering the curves in one diagram. Such a comparison of calculated and measured data is carried out in the reduced diagram as an example. Fig. 11 shows the correlation of the hover curves.

The calculated curve is valid for the average rotor Mach number of the flight tests (see chapter 4.1) allowing the results to be compared directly.

Deviations of the curves may have different reasons. Differences of  $K_{ps}$  with  $K_G=0$  could hint at an unprecise profile drag characteristic for the rotor blades as the induced power disappears in this range. The effects overlap when  $K_G$  is increased. In order to recognize the underlying causes parameter variations are necessary in the calculation program /22/. In this case, the curves intersect. The deviations are rather small; however, striking is the fact that the curves run up in a different way. In order to solve this problem it would be advisable to fly further hover points in a higher  $K_G$  range as the number of test points is actually too small here. Therefore, the tethered method of testing would be of advantage because high values of  $K_G$  with ground reference for the velocities can be flown. This method has not been applied for the tests carried out so far, but high  $K_G$  values were established by hovering in large heights.

In Fig. 12 the theoretical (calculated) powers are compared to the adjustment curves of the test data for forward flight with climb and descent.

When considering the curves for  $\bar{V}_v=0$ , differences can above all be found in the range of high velocities while there is a good accordance in the range of power minimum and below.

The early rise of the measured curve after power minimum could have its cause in an increased parasite drag of the test helicopter as a result of additional instruments on the helicopter. In this connection, the sensor of the velocity-measuring system LASSIE is concerned as well as a pod on the rotor head to examine rotor dynamics. The drag produced by these devices is not taken into account in the calculation program. Regarding the climb curves with  $\bar{V}_v=0.5$  and 1.0, the power differences are inverse. For this reason, the fuselage could be influential as well, for instance a separate flow region that vanishes again during climb.

An exacter investigation would necessitate a larger number of measuring points in the range of high velocity with climb and descent.

The second striking difference between the measured data on the one hand and the calculated data on the other concerns the range of small horizontal velocities with climb and descent. With the horizontal flight curve showing good correlation (except for the slightly steeper decrease with  $\bar{V}_h$ ), the differences grow with increasing vertical velocity.

In this situation, calculated power required is below the measured power, and this during climb as well as during descent. The largest difference arises from vertical autorotation resulting in the calculation between  $\bar{V}_v=-1$  and  $-1.5$  while in the tests values  $-1.5$  to  $-2.0$  were reached.

Deviations of this kind can only be referred to an inexact physical model for the calculation of the induced velocity of the rotor. In this case, the estimation makes use of the momentum theory which, however, does not describe the real conditions in the range of vertical climb and descent exactly enough. For this reason, empirically-ascertained correcting factors are entered in performance calculation programs. They have to be effective in the range mentioned above, however they are missing in the calculation model applied here.

Conclusions for our further investigations can be drawn from the graphical and thus clear comparison of calculated data on the one hand and reduced curves from the flight tests on the other. Parameter ranges result that due to the course of the regression curve that cannot be explained require a higher concentration of measuring points. On the other hand, conclusions can be drawn on the validity of the assumptions that had been made in the calculation program concerning physical effects of the helicopter. In doing so, an iterative proceeding is quite opportune so as to approach real conditions.

## 6. Summary

The determination and presentation of power required of a helicopter for forward flight with climb and descent is a system with six relevant and independent as well as one dependend influencing variable. With the help of the data reduction method, this system is to be reduced in a way that the number of points to be flown is decreased and a clear graphical presentation is made possible.

Non-dimensional parameters can be deduced from dimensional analysis, reducing the system in question here to 4+1 variables. Restriction to hover flight makes it possible to show power required as a family of curves in one diagram, neglecting only effects of minor importance. Extension to the forward flight with climb and descent is justified by adding physical information about the power parts. As a consequence, the influence of the velocities can be described with the help of a power factor. Such a division of the independent parameters allows a further-reaching reduction.

The test data worked out this way are presented numerically in a definite way by three-dimensional polynomes established through computations of an adjustment. Thereby, random errors are eliminated.

These characteristic fields can be made use of for a comparison with data from performance calculation programs. Plotting both of them in one diagram each allows a graphical comparison.

The characteristic fields defined by polynomes make it possible to calculate power required for certain flight states and thus enables an immediate performance calculation.

## 7. References

- /1/ H. Huber and G. Polz, Helicopter performance evaluation for certification, Ninth European Rotorcraft Forum, No. 26, September 1983
- /2/ K.T. McKenzie, Flight testing for performance and flying qualities, AGARD-LS-63-9, April 1973
- /3/ G.D. Padfield, Flight testing for performance and flying qualities, AGARD-LS-139-7, May 1985
- /4/ P. O'Hara, A method of performance reduction for helicopters, R&M No. 2770, 1947
- /5/ F.C. Kinchela, A comprehensive method of helicopter performance reduction, AHD Note 48, 1958
- /6/ I.J. Carter, An experimental assesment of the helicopter performance reduction method developed by Kinchela; AHD Note No. 51, 1961
- /7/ G.F. Langdon, A note on performance reduction for helicopters fitted with gasturbine engines with free power turbines and torquemeters, A&H Note No. 53, 1961
- /8/ G.F. Langdon, Experimental methods for helicopter performance reduction, A.H.D Note 54, AAEE Boscombe Down, 1961
- /9/ I.A. Fisher, The measurement and prediction from flight test results of a helicopter's vertical climb performance using a non-dimensional method, AAEE/Res/310, Jan. 1964, Boscombe Down
- /10/ Knowles, The application of non-dimensional methods to the planning of helicopter performance flight trials and the analysis of results, ARC CP 927, 1967
- /11/ Engineering Science Data Unit, Introduction to non-dimensional methods for the measurement of performance of turbine-engined helicopters, ESDU 73026
- /12/ Engineering Science Data Unit, Non-dimensional methods for the measurement of hover performance of turbine-engined helicopters, ESDU 73027
- /13/ Engineering Science Data Unit, Non-dimensional methods for the measurement of level-flight performance of turbine-engined helicopters, ESDU 74042
- /14/ B.H. Boirun, Generalizing helicopter flight test performance data (GENFLT), 34th Annual National Forum of the American Helicopter Society, No. 78-44, May 1978
- /15/ E.H. Smith, An empirical prediction method for helicopter performance in low speed level flight and in vertical and forward flight climbs, Sixth European Rotorcraft and Powered Lift Aircraft Forum, No. 53, September 1980
- /16/ I.S. Hayden, The effect of the ground on helicopter hovering power required, 32th AHS Forum, May 1976

- /17/ I.C. Cheeseman, W.E. Bennett, The effect of the ground on a helicopter rotor in forward flight, AAE Report, Reports and Memoranda No. 3021, 1955
- /18/ L.I. Sedov, Similarity and dimensional methods in mechanics, Academic Press Inc., Infosearch LTD, 1959
- /19/ I. Zierep, Ähnlichkeitsgesetze und Modellregeln der Strömungslehre, G. Braun Verlag, Karlsruhe, 1982
- /20/ H. Schlichting, Grenzschicht-Theorie, G. Braun Verlag, Karlsruhe, 1965
- /21/ R.C. Binder, Fluid mechanics, 4th Edition, Prentice-Hall, Inc., Englewood Cliffs, N.J., 1962
- /22/ J.M. Drees, The art and science of rotary wing data correlation, JAHS July 1976

Occurring Exponents of \ Influencing Variables	mg	U	V <sub>h</sub>	V <sub>v</sub>	ρ	a	R	P
Mass Unit [kg]	1	0	0	0	1	0	0	1
Length Unit [m]	1	1	1	1	-3	1	1	2
Time Unit [s]	-2	-1	-1	-1	0	-1	0	-3

Table 1: Exponents of Units in the Influencing Variables

No.	Parameter	Abbreviation	Name
1	$\frac{mg}{\frac{\rho}{2} U^2 S}$	= K <sub>G</sub>	Weight Coefficient *
2	$\frac{V_h}{U}$	= λ <sub>h</sub>	Horizontal Advance Ratio
3	$\frac{V_v}{U}$	= λ <sub>v</sub>	Vertical Advance Ratio
4	$\frac{U}{a}$	= Ma <sub>U</sub>	Mach Number of the Blade Tip
5	$\frac{P}{\frac{\rho}{2} U^3 S}$	= K <sub>P</sub>	Power Coefficient *
	* with S = π R <sup>2</sup> (Rotor Disc Area)		

Table 2: Non-Dimensional Parameters

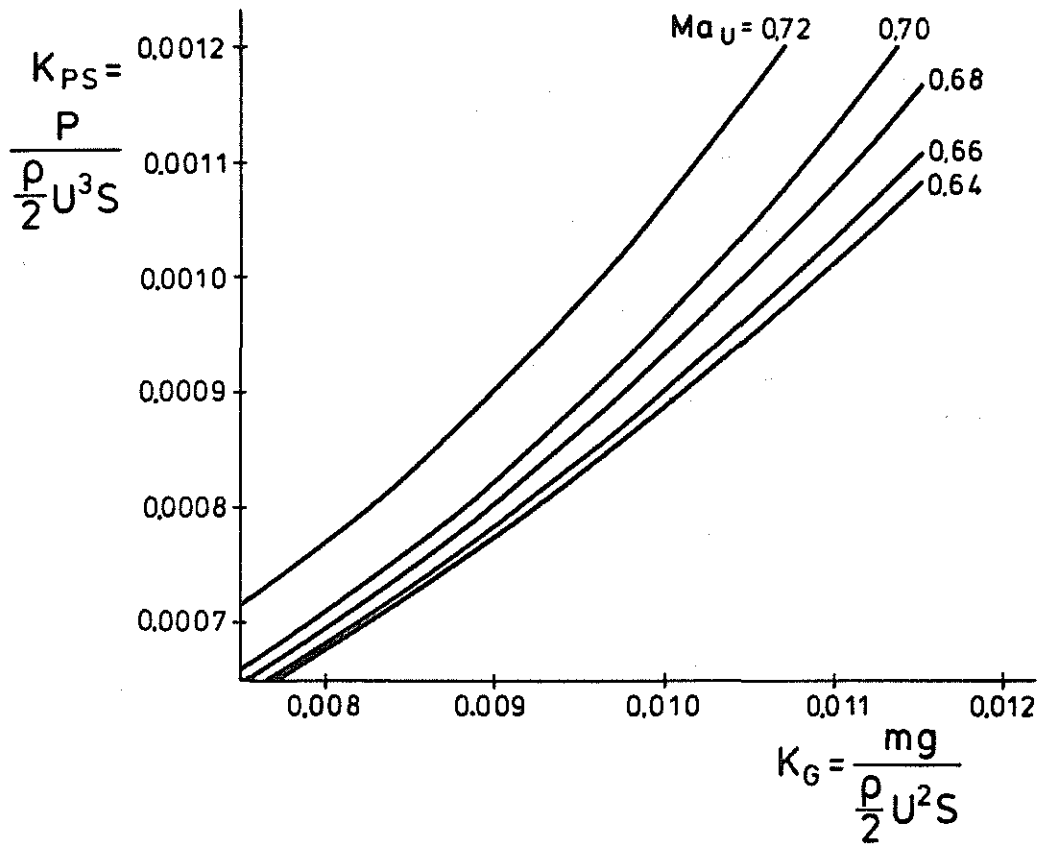


Figure 1: Power Required in Hover

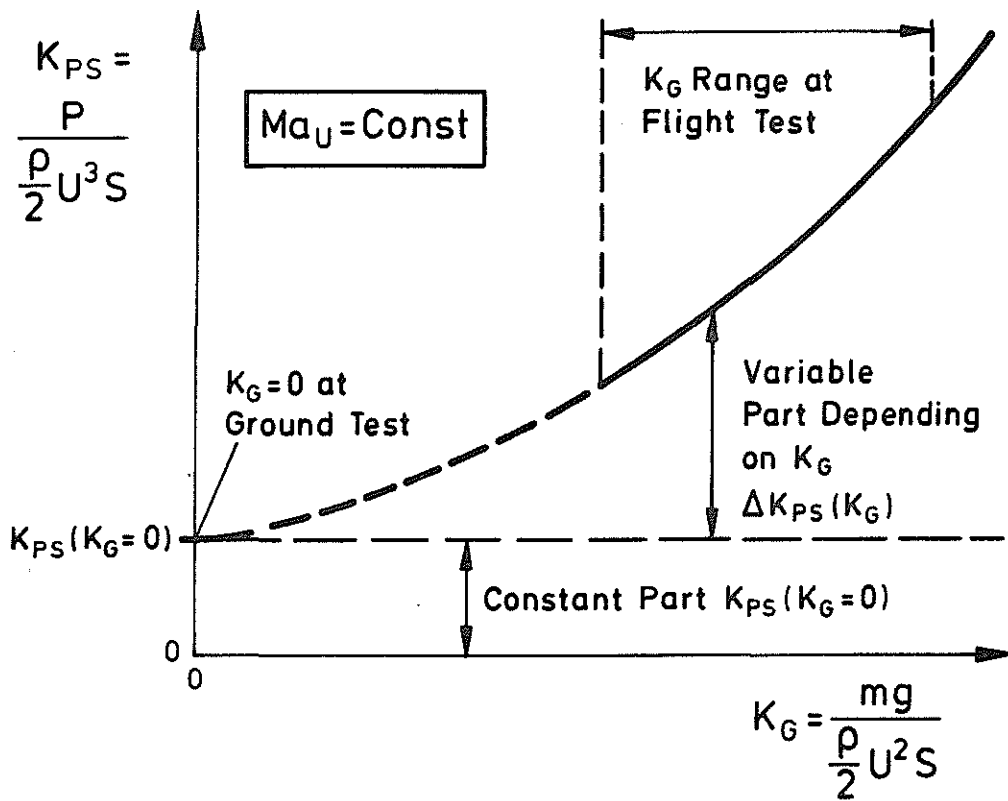


Figure 2: Division of Power Required in Hover

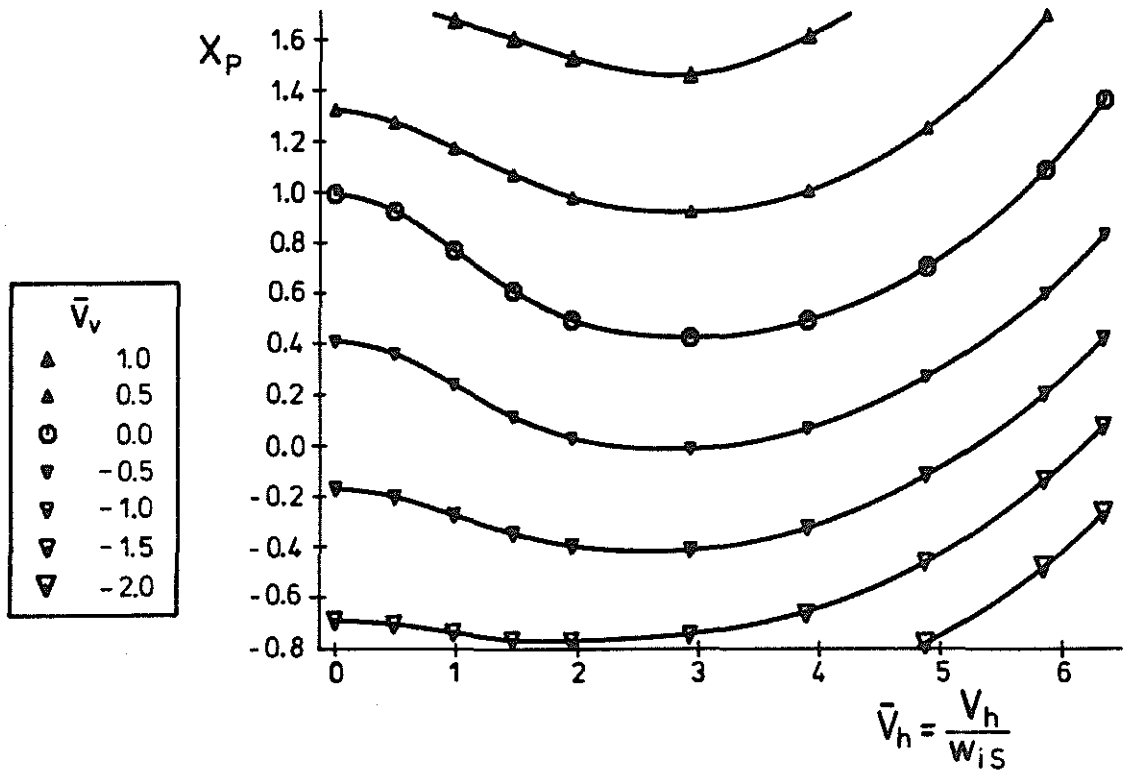


Figure 3: Power Factor for Forward Flight Climb and Descent

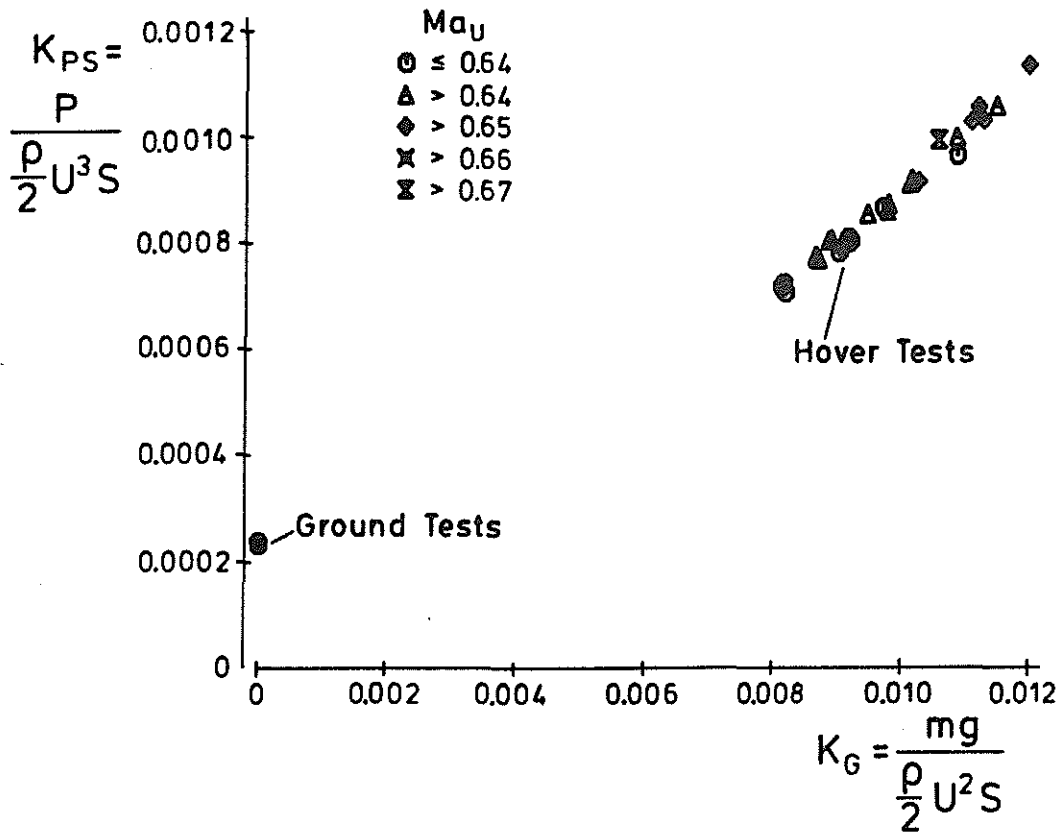


Figure 4: Data from Hover and Ground Tests

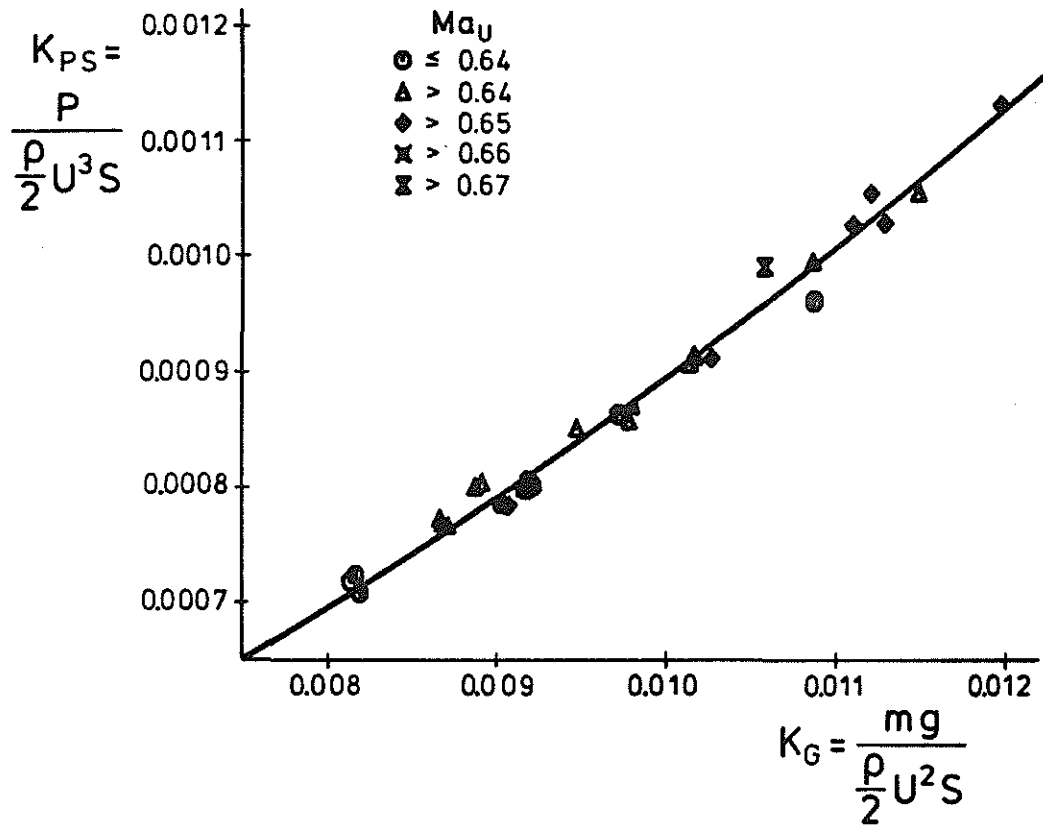


Figure 5: Curve of Adjustment to Hover Test Points

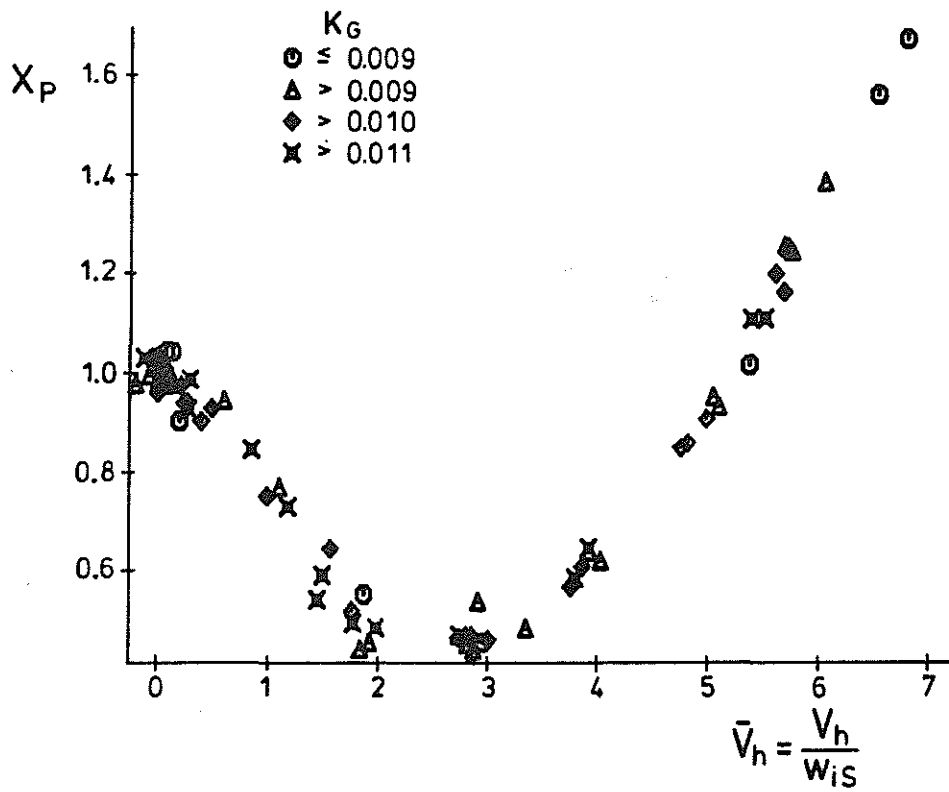


Figure 6: Power Factor in Horizontal Flight



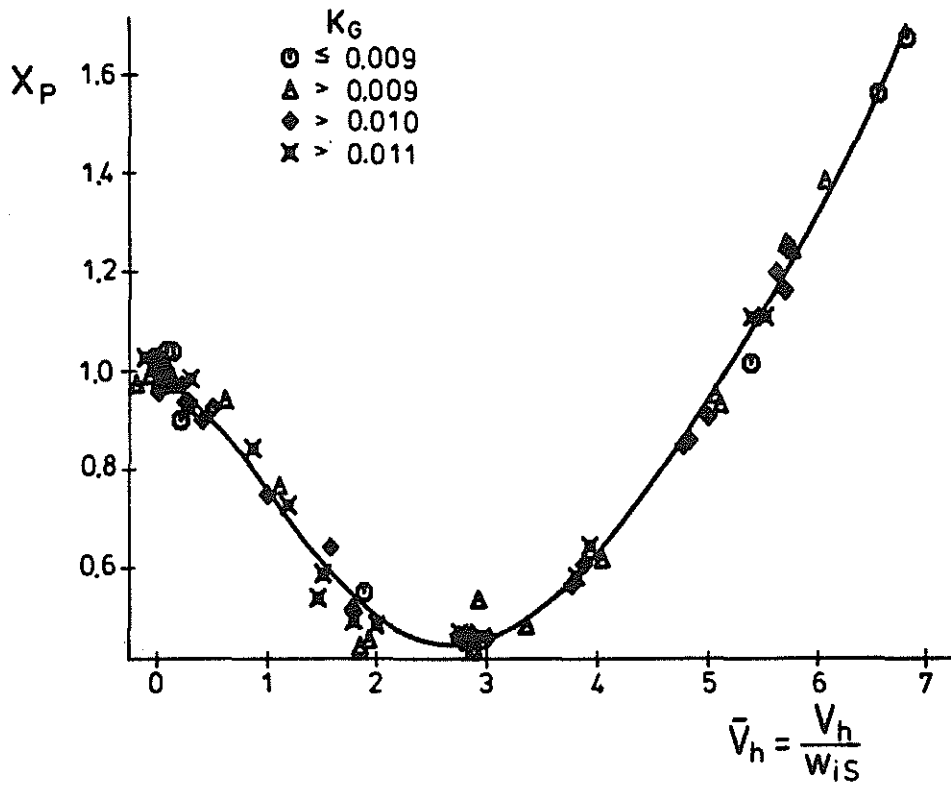


Figure 7: Curve of Adjustment to Horizontal Test Points

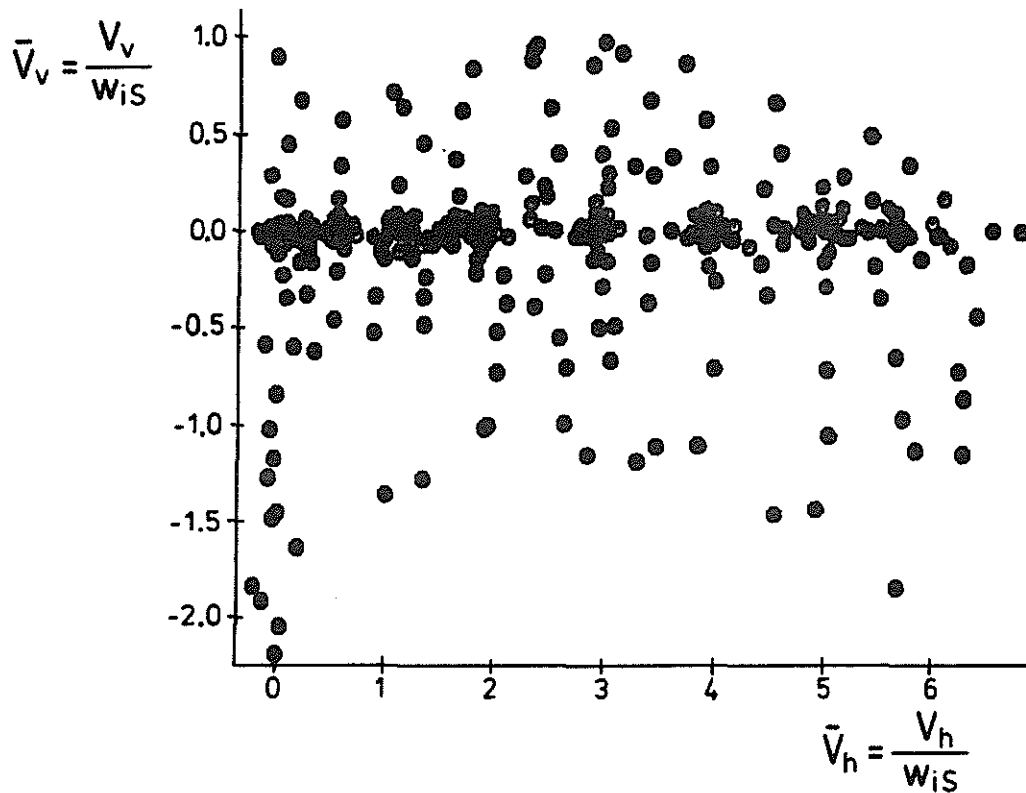


Figure 8: Combinations of  $\bar{V}_h$  and  $\bar{V}_v$  at Flight Test

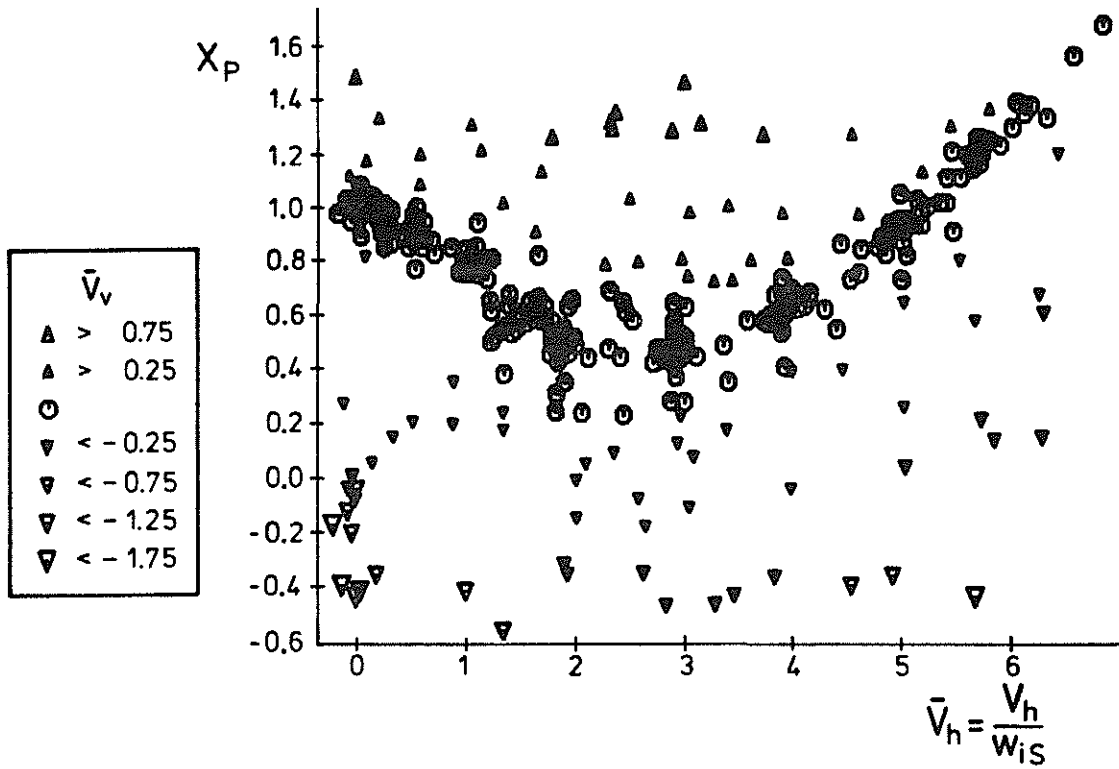


Figure 9: Power Factors from Flight Tests as a Function of  $\bar{V}_h$  and  $\bar{V}_v$

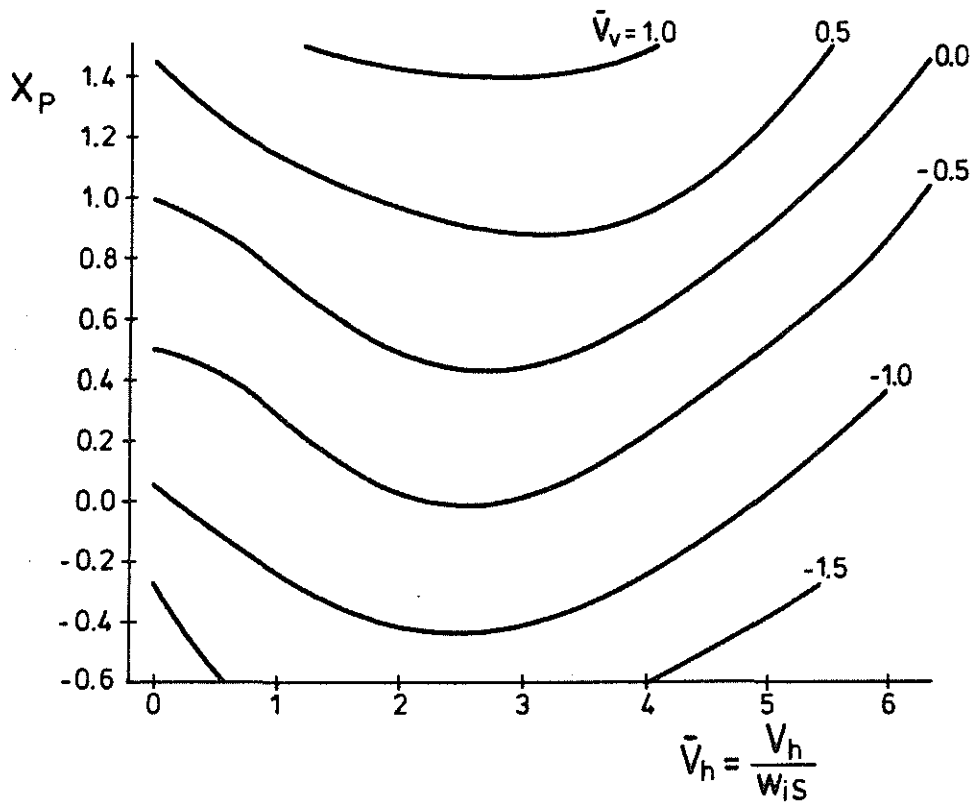


Figure 10: Regression Calculation for Forward Flight Climb and Descent

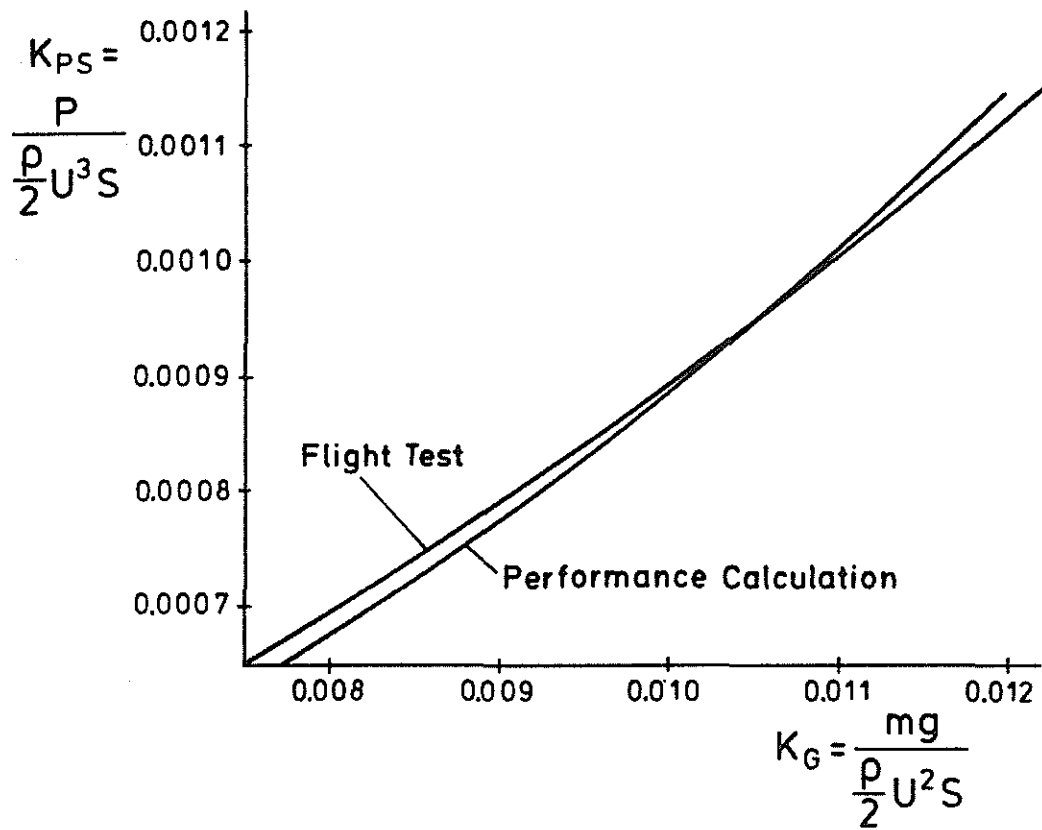


Figure 11: Correlation of Power Required in Hover

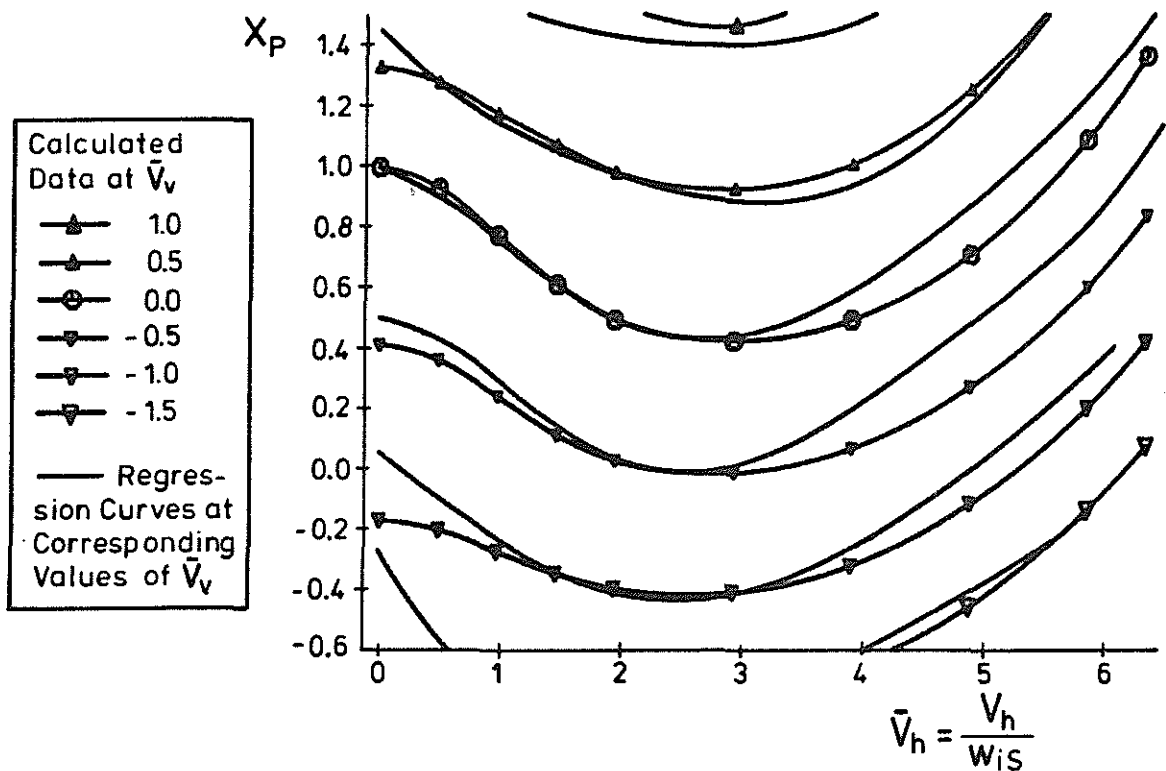


Figure 12: Correlation of Regression Curves to Calculated Data for Forward Flight Climb and Descent